

# Speciation and distribution of copper in a mining soil using multiple synchrotron-based bulk and microscopic techniques

Jianjun Yang · Jin Liu · James J. Dynes · Derek Peak · Tom Regier · Jian Wang · Shenhai Zhu · Jiyan Shi · John S. Tse

Received: 17 June 2013 / Accepted: 2 October 2013 / Published online: 30 October 2013  
© Springer-Verlag Berlin Heidelberg 2013

**Abstract** Molecular-level understanding of soil Cu speciation and distribution assists in management of Cu contamination in mining sites. In this study, one soil sample, collected from a mining site contaminated since 1950s, was characterized complementarily by multiple synchrotron-based bulk and spatially resolved techniques for the speciation and distribution of Cu as well as other related elements (Fe, Ca, Mn, K, Al, and Si). Bulk X-ray absorption near-edge structure (XANES) and extended X-ray absorption fine structure (EXAFS) spectroscopy revealed that soil Cu was predominantly associated with Fe oxides instead of soil organic matter. This agreed with the closest association of Cu to Fe by microscopic X-ray fluorescence (U-XRF) and scanning transmission X-ray microscopy (STXM) nanoanalysis, along with the non-occurrence of photoreduction of soil Cu(II) by quick Cu L<sub>3,2</sub>-edge XANES spectroscopy

(Q-XANES) which often occurs when Cu organic complexes are present. Furthermore, bulk-EXAFS and STXM-coupled Fe L<sub>3,2</sub>-edge nano-XANES analysis revealed soil Cu adsorbed primarily to Fe(III) oxides by inner-sphere complexation. Additionally, Cu K-edge  $\mu$ -XANES, L<sub>3,2</sub>-edge bulk-XANES, and successive Q-XANES results identified the presence of Cu<sub>2</sub>S rather than radiation-damage artifacts dominant in certain microsites of the mining soil. This study demonstrates the great benefits in use of multiple combined synchrotron-based techniques for comprehensive understanding of Cu speciation in heterogeneous soil matrix, which facilitates our prediction of Cu reactivity and environmental fate in the mining site.

**Keywords** Copper · XANES · EXAFS · XRF · STXM · Mining soil · Molecular speciation · Radiation damage

Responsible editor: Stuart Simpson

**Electronic supplementary material** The online version of this article (doi:10.1007/s11356-013-2214-8) contains supplementary material, which is available to authorized users.

J. Yang · J. Liu · S. Zhu · J. Shi (✉)  
Department of Environmental Engineering, Zhejiang University,  
866 Yuhangtang Road, Hangzhou, Zhejiang 310058,  
People's Republic of China  
e-mail: shijiyang@zju.edu.cn

J. Yang · J. S. Tse (✉)  
Department of Physics and Engineering Physics, University of  
Saskatchewan, 116 Science Building, Saskatoon, SK S7N 5E2,  
Canada  
e-mail: john.tse@usask.ca

J. J. Dynes · T. Regier · J. Wang  
Canadian Light Source Inc., University of Saskatchewan, Saskatoon,  
SK S7N 0X4, Canada

D. Peak  
Department of Soil Science, University of Saskatchewan, Saskatoon,  
SK S7N 5A8, Canada

## Introduction

Soil Cu contamination as a side effect of mining activities is an increasing concern as a result of the growing global Cu demand (Elguindi et al. 2011). It is generally accepted that molecular-level knowledge about chemical species of heavy metals in soils will advance our ability to predict their reactivities and environmental fates (Manceau et al. 2002; Hesterberg et al. 2011). The capability and versatility of synchrotron-based techniques in performing molecular-scale speciation of soil heavy metals are well established (Manceau et al. 2002; Brown et al. 2005). However, fully characterizing the speciation of Cu in contaminated soils is challenging, as many Cu absorbents, such as minerals (Fe oxides, Mn oxides, clays, etc.) and soil organic matter (SOM), are often present in a single soil sample. Previous molecular-scale studies mainly focused on Cu-contaminated agricultural soils and concluded that Cu was primarily associated with SOM rather than with mineral sorbents (Flogeac et al. 2004; Boudesocque et al.

2007; Jacobson et al. 2007; Strawn and Baker 2008, 2009). Recently, laboratory-based sequential extraction analysis has shown dominant association of Cu to soil minerals in some mining soils (Favas et al. 2011). These contrasting results highlight the need for further molecular-level characterization of Cu speciation in mining soils to improve predictions of Cu behavior in contaminated mining sites. Furthermore, soils are heterogeneous assemblages of diverse soil particles of sizes that typically range from <2-mm sand grains to nanometer-sized clay particles; all of these particles are potential sites for metal sequestration in contaminated soils, and thus, the distribution and speciation of soil heavy metals vary on similar spatial scales to those of the soil minerals (Hesterberg et al. 2011). Therefore, besides bulk lab and spectroscopic-based soil Cu speciation, the microscale distribution and speciation of Cu in mining soils also need further characterization.

Synchrotron-based Cu K-edge X-ray absorption near-edge structure (XANES) and X-ray absorption fine structure (EXAFS) spectroscopy have been widely utilized in soil systems to perform chemical speciation, as these two techniques can provide average oxidation state and local structural information (interatomic distances, coordination numbers, and bond disorder), respectively (Liu and Wang 2004; Strawn and Baker 2009). However, EXAFS cannot easily distinguish the first shell of Cu–O from Cu–N due to similar backscattering contribution of O and N (Shi et al. 2008). This is significant because functional groups with O- or N-absorbing sites of SOM are both possible neighbors in Cu–ligand structures likely present in soils (Frenkel et al. 2000; Croue et al. 2003). In contrast, Cu L<sub>3,2</sub>-edge XANES spectroscopy probes the dipole-allowed Cu 2p→3d electron transitions, which is more sensitive to the ligand field surrounding Cu (Yang et al. 2011) and can readily distinguish between Cu–O and Cu–N metal–ligand bonds (Shimizu et al. 2001). Compared to K-edge, Cu XANES spectra at L<sub>3,2</sub>-edge exhibits much sharper spectral features, which results in advantages in characterizing soil Cu oxidation state and bond valency (Schofield et al. 1995), especially for low-abundance Cu species in contaminated soils. Therefore, a combined application of Cu K-edge EXAFS and L<sub>3,2</sub>-edge XANES provides a thorough measurement of bulk soil Cu speciation.

Bulk-XANES and EXAFS spectroscopy (approximately millimeter level) represent the average speciation of heavy metals in contaminated soils, which may thus obscure speciation information of components present in low abundance. Therefore, spatially resolved microscopic X-ray fluorescence (μ-XRF) and scanning transmission X-ray microscopy (STXM) spectroscopy are increasingly employed in soil research (Wan et al. 2007; Fittschen and Falkenberg 2011). The μ-XRF, coupled with μ-XANES spectroscopy, has been used to investigate the distribution and speciation of soil Cu at the micro-scale (Strawn and Baker 2008, 2009). This technique, using hard X-ray beam (typically 5–20 keV), is suitable for most metal contaminants and mineral elements (e.g., Fe, Mn,

Ca, and K) (Strawn and Baker 2008, 2009). Although clays greatly affect the distribution of Cu (Morton et al. 2001), clay minerals contain primarily low-Z elements Al and Si that are usually inaccessible to μ-XRF analysis. This limits studies of the interaction of Cu with clays in soils using X-ray microprobes. In contrast, STXM, using soft X-ray beam (<2,500 eV), covers the energies of Al and Si K-edges and Cu L-edges (Wan et al. 2007), making it ideal to investigate the interactions of Cu with soil clays. Additionally, STXM, coupled with XANES spectroscopy, has a high spatial resolution at the nano-scale (30–50 nm) (Wan et al. 2007; Lawrence et al. 2012), which facilitates probing the nano-scale distribution and speciation of soil Cu. Consequently, a much deeper understanding of the heterogeneous distribution and speciation of soil Cu at micro- and nano-scales may be achieved by a combination of μ-XRF and STXM analysis.

The flux and brilliance of X-rays produced from modern synchrotrons greatly enhance the capacities of synchrotron-based speciation of heavy metals in contaminated soils (Manceau et al. 2002). However, radiation damage due to high-brightness beam may also result in fast photoreduction of organic Cu(II) complexes on the time scale of the XANES measurements (Strawn and Baker 2009; Manceau and Matynia 2010; Yang et al. 2011), thus complicating the interpretation of soil Cu valency according to XANES fingerprint analysis. Therefore, radiation damage should be considered as a potential source of low oxidation state Cu in contaminated soils where soil organic Cu(II) complexes are present. As radiation damage depends on the radiation dose received by the targeted samples (Yang et al. 2011), quick XANES spectroscopy with reduced beam dwell time for each XANES measurement should not only minimize radiation damage, but also aid in diagnosing the occurrence of radiation-induced spectral changes.

Taking one single mining soil from a long-term contaminated mining site as an example, the objectives of this study were (1) to investigate the complementary molecular speciation of Cu in the mining soil employing Cu K-edge bulk-XANES and bulk-EXAFS and L<sub>3,2</sub>-edge bulk-XANES; (2) to reveal the micro- and nano-scale distribution and speciation of soil Cu using μ-XRF coupled with Cu K-edge μ-XANES spectroscopy and STXM with Cu/Fe L-edge and Al/Si K-edge XANES spectromicroscopy, respectively; and (3) to determine the extent of radiation-induced photoreduction of Cu by quick Cu L<sub>2,3</sub>-edge XANES spectroscopy (Q-XANES).

## Material and methods

### Soil sample

The mining soil was collected at an abandoned Cu mine site in Zhuji County of Zhejiang Province, China (120°22'33.0" E,

29°36'39.1" N). This region is characterized by a subtropical monsoon climate with annual average temperature of ~16 °C and annual rainfall of ~1,335 mm. Mining activities began onsite in the 1950s and ended more than 20 years ago. The mining soil was classified as an Ultisol according to USDA soil taxonomy (USDA 1988). According to our previous study (Chen et al. 2006), the mining site has particularly high Cu concentration, up to ~12,700 mg kg<sup>-1</sup> Cu. The soil sample was collected from the surface horizon (0–20 cm) of a selected representative area using compositing technique, air-dried and then ground to pass through a 2-mm nylon sieve, homogenized, and stored for subsequent analyses. The pH, cation exchange capacity (CEC), the total organic carbon (TOC), total carbonates, and total metal contents (Cu/Al/Fe/Mn) of the soil were determined following the standard methods recommended by the Chinese Society of Soil Science (Lu 1999). Soil mineral composition was measured by XRD (Rigaku D/MAX 2550/PC, Japan). The selected physico-chemical properties of the mining soil are compiled in Table 1. Notably, the soil chosen has low SOM content, which represents typical feature of soils collected at mining sites (Boularbah et al. 2006; Guo et al. 2011).

Cu K-edge bulk-XANES/EXAFS spectroscopy

The Cu K-edge bulk-XANES/EXAFS measurements were conducted in ambient conditions at beamline BL14W1 at the Shanghai Synchrotron Radiation Facility (SSRF), China. The operating conditions of the storage ring in SSRF were 3.5 GeV and a maximum current of 300 mA. All the measurements were collected under unfocused mode, with an estimated size of beam spot as ~3 mm, using a liquid nitrogen gas-cooled double crystal monochromator using Si (311) crystals and a harmonic rejection mirror. The soil sample (<0.04 mm), Cu adsorbed on goethite (paste) and Elliot humic acid (HA, wet), and Cu nitrate (liquid) were measured in partial fluorescence yield mode using a four-element silicon drift detector (Bruker's XFlash® QUAD 5040, Germany). The other Cu references, diluted with boron nitride (99.5 %, Alfa Aesar, Ward Hill, MA), were collected in transmission mode. All spectra were calibrated to the inflection point of Cu K-edge at 8,979 eV, using a Cu foil measured in transmission

mode. Multiple XANES and EXAFS measurements were averaged to obtain adequate signal-to-noise ratio and to verify that radiation damage was not occurring over the time scale of the experiment on the same spot for each sample. The XANES data processing, including linear combination fitting (LCF) analysis, was conducted using Athena (8.050), while EXAFS data analysis were processed by Athena and Artemis (8.050) (Ravel and Newville 2005). Further experimental details and data processing are described in the Supplementary Materials.

Cu L<sub>3,2</sub>-edge bulk-XANES spectroscopy

The Cu L<sub>3,2</sub>-edge bulk-XANES spectra of inorganic Cu references (CuO, Cu, Cu<sub>2</sub>O, Cu<sub>2</sub>S, and CuS) were collected at the Spherical Grating Monochromator (SGM) beamline 11ID-1 of the Canadian Light Source (CLS) in Canada (Regier et al. 2007). Cu L<sub>3,2</sub>-edge spectra of Cu(II) acetate, Cu phthalocyanine, and the mining soil were collected at the Soft X-ray beamline 4B7B at the Beijing Synchrotron Radiation Facility (BSRF) in China instead of the SGM beamline of CLS, to avoid radiation damage of organic Cu(II) complexes due to its high beam intensity (~10<sup>12</sup> photons/s) compared to beamline 4B7B (~10<sup>8</sup> photons/s) in BSRF (Yang et al. 2011). The sizes of beam spot at the SGM beamline of CLS and Soft X-ray beamline of BSRF were set to be ~30 μm and ~1 mm, respectively. The energy ranges and steps of the scans for Cu L<sub>3,2</sub>-edge XANES spectra were set following our previous study (Yang et al. 2011). Powder soil sample (<0.04 mm) and all the Cu references were mounted on the double-sided conductive carbon tape for the measurement of Cu L<sub>3,2</sub>-edge XANES spectra in ambient temperature. All the spectra were collected in total electron yield (TEY) mode and scanned at least twice. Good reproducibility of the repeated successive measurements indicated that photoreduction of inorganic and organic Cu(II) compounds did not occur. The pressure was kept below 1 × 10<sup>-7</sup> Torr during the measurements due to UHV requirements of the beamline; to avoid sample chamber contamination, the Cu adsorption references (on goethite and HA) that contained liquid water were not measured with this technique. Further data processing is described in the Supplementary Materials.

**Table 1** Selected physicochemical properties of the soil used in the study

Soil type	pH (1:2.5)	TOC <sup>a</sup> (%)	CEC <sup>b</sup> (cmol kg <sup>-1</sup> )	T-Cu <sup>c</sup> (g kg <sup>-1</sup> )	T-Al <sup>c</sup> (g kg <sup>-1</sup> )	T-Fe <sup>c</sup> (g kg <sup>-1</sup> )	T-Mn <sup>c</sup> (g kg <sup>-1</sup> )	Mineral composition
Ultisol	5.87	0.55	5.35	5.08	10.2	121	13.0	Quartz, kaolinite, clinocllore, muscovite

<sup>a</sup> Total organic carbon content

<sup>b</sup> Cation exchange capacity

<sup>c</sup> Total Cu/Al/Fe/Mn contents

### $\mu$ -XRF/XANES microanalysis

The  $\mu$ -XRF/XANES experiments were conducted in ambient conditions at SSRF beamline 15U. Monochromatic X-rays with 10 keV photon energy were generated by a Si (111) crystal monochromator and focused to a measured spot size of  $5 \times 5 \mu\text{m}^2$  using a Kirkpatrick–Baez mirror system. A thin soil section ( $\sim 60 \mu\text{m}$  thickness) was mounted on the seven-axis sample stage under the observation of a microscope. A selected sample area ( $0.350 \times 0.075 \text{ mm}$ ) was scanned in step size of  $5 \mu\text{m}$ , and fluorescence signals of Cu, Fe, Mn, K, and Ca were selectively acquired with the dwell time of 1.5 s using a one-element Si drift detector (Vortex-EX, SII NanoTechnology Inc.). Immediately after XRF mapping, image processing of the  $\mu$ -XRF spectra for each individual element was performed using Igor Pro 6.0 software (IGOR) and then Cu K-edge  $\mu$ -XANES spectra were collected on interesting spots observed in IGOR. Due to detection limits (estimated as  $\sim 4,000 \text{ mg kg}^{-1}$ ), only Cu hot spot 1 but moderate spot 2 and spot 3 succeed in spectrum collection. Three scans were averaged to produce a merged spectrum with acceptable signal-to-noise ratio for further analysis. Further experimental details and data processing are described in the Supplementary Materials.

### STXM nanoanalysis

X-ray imaging and spectromicroscopy were carried out at the CLS using the STXM microscope at the spectromicroscopy beamline 10ID-1 (Yang et al. 2011). Soil microaggregates ( $< 0.04 \text{ mm}$ ), sieved from the mining soil, were dispersed in Millipore water and then deposited onto a silicon nitride window (thickness 100 nm, Norcada Inc.). After air drying, the mounted soil sample was transferred to the helium-filled chamber for STXM measurements in ambient temperature. Sequences of images (i.e., stacks) based on spatially resolved X-ray transmission were collected at the Cu and Fe L-edges and the Al and Si K-edges and converted to optical density images by normalization using the incident flux through a region of the silicon nitride window devoid of soil particles. The quantitative Cu, Fe, Al, and Si component maps were generated following the procedures reported by Dynes et al. (2006), using previously reported reference spectra (Hitchcock et al. 2009; Lawrence et al. 2012). Further experimental details and data processing are described in the Supplementary Materials.

### Diagnosis of radiation damage effect by Q-XANES spectroscopy

The occurrence of radiation damage depends on the radiation dose received by the targeted samples under X-ray exposure, which can generally be estimated by beam intensity. In this

study, the observation of soil Cu(I) species (see “Results”) and the possible association of photo-reducible Cu(II) humic acid complexes in the mining soil made it important to assess the potential for radiation-induced Cu(II) reduction to determine whether the observed soil Cu(I) was a true chemical species rather than an artifact from radiation damage. This is especially important in our experiments because Strawn and Baker (2008) found that radiation damage induced photoreduction of organic Cu(II) complexes to Cu(I) in a contaminated soil during  $\mu$ -XANES measurement with similar X-ray beam intensity ( $\sim 10^{10}$  photons/s) to our  $\mu$ -XANES experiment at 15U beamline of SSRF with beam intensity of  $\sim 10^{10}$  photons/s. Our recent study indicated that a reduction of beam intensity could minimize or eliminate photoreduction of organic Cu(II) complexes (Yang et al. 2011). Therefore, we utilized a quick-scan mode (20 s) instead of normal scan (5 min) for Cu  $L_{3,2}$ -edge XANES measurements (Q-XANES) at the CLS SGM beamline. Each quick scan decreased the radiation dose by about  $\sim 15$  times compared to normal scan. If we put each quick and normal scan in the same time scale, the beam intensity for each quick scan should be  $\sim 10^{10}$  photons/s calculated from the beam intensity of normal scan ( $\sim 10^{12}$  photons/s). Such Q-XANES spectroscopy gained comparable X-ray intensity to  $\mu$ -XANES experiment at 15U in SSRF, which makes diagnosing radiation damage effects possible to measure by gradual spectrum changes in successive scans.

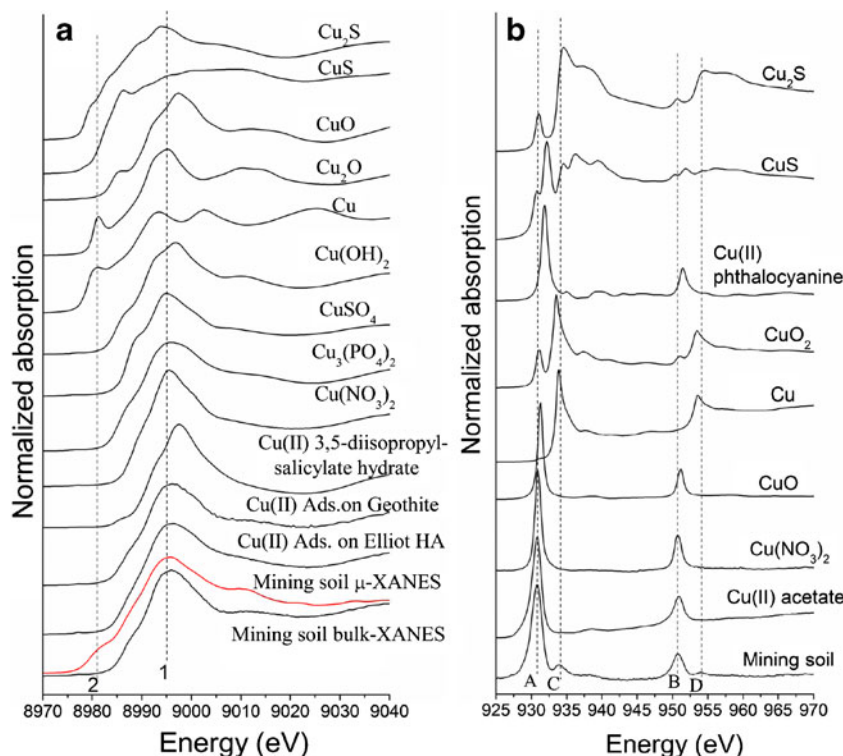
For the SGM measurements, the mining soil was mixed with Millipore water and deposited onto Au-coated Si wafers, air dried, and examined by Q-XANES at the Cu L-edge. Nineteen successive quick scans were conducted on the same spot of the mining soil to collect the Q-XANES spectra in the TEY mode. The size of beam spot, the energy range, and step size for each scan were kept the same as the normal XANES measurement at this beamline (see “Cu  $L_{3,2}$ -edge bulk-XANES spectroscopy” section for details). Further data processing is described in the Supplementary Materials.

## Results

### Cu K-edge and $L_{3,2}$ -edge Bulk-XANES analysis

The Cu K-edge and  $L_{3,2}$ -edge bulk-XANES spectra of the mining soil and references are shown in Fig. 1. The main peak (peak 1) at around 8,995 eV resulted from the Cu  $1s$  to  $4p_z$  and  $4p_{x/y}$  electron transitions (Fig. 1a) (Strawn and Baker 2008). Splitting of this main peak, arising from anisotropic symmetry of Cu(II) compounds (Jahn–Teller distortion) (Liu and Wang 2004), resulted in two different inflections corresponding to peak  $\alpha$  and peak  $\beta$ , as indicated in the first derivative spectra of soil Cu in Fig. S1 provided as Supplementary Material (SM). The energy separation and intensity of the peak  $\alpha$  and

**Fig. 1** The Cu K-edge (a) and L<sub>3,2</sub>-edge (b) XANES spectra of the mining soil and Cu references. Red line and black line of the mining soil represent Cu K-edge  $\mu$ -XANES and bulk-XANES spectra of the mining soil. Spectral peaks of interest are marked by vertical dashed lines and labeled from 1 to 2 in (a) and from A to D in (b)



peak  $\beta$  depend on molecular composition and coordination, which has been used for qualitative soil Cu speciation (Strawn and Baker 2009). Energy separation of peak  $\alpha$  and peak  $\beta$  of soil Cu almost matched to that of Cu(II) adsorbed on goethite and Elliot HA rather than Cu(II) 3,5-diisopropylsalicylate hydrate, Cu(NO<sub>3</sub>)<sub>2</sub>, Cu<sub>3</sub>(PO<sub>4</sub>)<sub>2</sub>, CuSO<sub>4</sub>, Cu(OH)<sub>2</sub>, CuS, Cu<sub>2</sub>O, Cu, and CuO (Fig. S1 in SM). This suggested Cu(II) adsorbed on Fe oxides and soil organic matter were probably the end members of Cu in the soil. Another feature (peak 2) at about 8,980 eV was only observable in Cu, Cu<sub>2</sub>S, and Cu<sub>2</sub>O references, but not in the soil spectrum, suggesting only Cu(II) in the mining soil. Furthermore, according to the best LCF results of soil bulk-XANES spectra (Table 2 and Fig. S2 in SM), the majority of Cu was present as Cu(II) adsorbed on goethite (81.0 % of total Cu), whereas a minor fraction of Cu existed as Cu(NO<sub>3</sub>)<sub>2</sub> (16.7 % of total Cu) that may be a proxy for outer-sphere Cu complexes, along with a trace amount of Cu as Cu<sub>2</sub>S (2.3 % of total Cu).

Cu L<sub>3,2</sub>-edge XANES spectra were used to probe the associated covalent ligands and the oxidation state of soil Cu

(Fig. 1b). Two main sharp peaks were resolved from 930.7 to 932.2 eV (peak A, L<sub>3</sub>-edge) and from 950.9 to 951.9 eV (peak B, L<sub>2</sub>-edge) for Cu(II) references, and from 933.5 to 934.6 eV (peak C) and from 953.5 to 954.6 eV (peak D) for Cu(0)/Cu(I) references, respectively. Peaks A and B of the Cu(II) references were due to the transitions of Cu 2p<sub>3/2</sub> and 2p<sub>1/2</sub> to Cu 3d<sup>9</sup> unoccupied states, respectively, while peaks C and D of Cu(0)/Cu(I) references arose from the transitions of Cu 2p<sub>3/2</sub> and 2p<sub>1/2</sub> to Cu 3d<sup>10</sup>4s unoccupied states, respectively (Grioni et al. 1989). Peak A of all the Cu(II) compounds with oxygen ligand, resolved at 930.8~931.2 eV, is located at the lower energy side of that for Cu(II) phthalocyanine with Cu–N bond at 931.9 eV (Fig. 1b). Similar behavior was also observed in the peak B which was resolved at 950.8~951.1 eV for references with Cu(II)–O bond and at 951.5 eV for Cu(II) phthalocyanine (Fig. 1b). These shifts of edge peaks for Cu(II) compounds to higher energy were interpreted as the decreased electronegativity of the bonding ligand in the order O < N (Shimizu et al. 2001). The occurrence of peak A in the reference spectra of Cu<sub>2</sub>O and Cu<sub>2</sub>S was attributed to CuO

**Table 2** Linear combination fitting results of Cu K-edge XANES showing the relative percent ( $\pm$ standard deviation) of each Cu species in the bulk soil and soil microaggregate of Cu hot spot 1

Soil	Goodness of fit		Percentages of targeted components		
	R factor	$\chi^2$	Cu ads. on goethite (%)	Cu(NO <sub>3</sub> ) <sub>2</sub> (%)	Cu <sub>2</sub> S (%)
Bulk soil	0.001	0.157	81.0 $\pm$ 6.3	16.7 $\pm$ 4.8	2.3 $\pm$ 7.9
Cu hot spot	0.002	0.234	42.2 $\pm$ 2.0	–	57.8 $\pm$ 2.2

impurity (Grioni et al. 1989), which probably also accounted for the spurious pre-edge peak of CuS observed in this study, but absent in a previous study reported by Grioni et al. (1989). For the mining soil, the presence of strong peak A at 930.9 eV and peak B at 950.9 eV in the Cu  $L_{3,2}$ -edge bulk-XANES spectra indicated the dominance of soil Cu(II) (Fig. 1b), consistent to Cu K-edge bulk-XANES analysis (Fig. 1a). The energy positions of these two peaks in the soil spectra were consistent with references with Cu(II)–O bonding (Fig. 1b), which implied Cu(II) probably mainly binds to soil components through Cu–O rather than Cu–N and Cu–S bonds. Moreover, two small peaks were observed at 933.9 and 954.1 eV in the Cu  $L_{3,2}$ -edge bulk-XANES spectrum of the mining soil (Fig. 1b). These two peaks almost matched peaks C and D in Cu(0)/Cu(I) references, which suggested the presence of some Cu species with low valency in the mining soil.

#### Cu K-edge bulk-EXAFS analysis

The EXAFS spectra of Cu K-edge (Fig. 2) were further fitted to theoretical scattering paths to provide more details on the soil Cu speciation. The Fourier transformed (FT) spectra of organic Cu compounds all contained two peaks at relatively long distance (3.0–3.5 Å) (Fig. 2b), and these peaks were considered to arise from the multiple scattering effects of Cu–O–C groups in soil organic Cu complexes (Karlsson et al. 2006). The lack of these peaks in the soil Cu spectrum qualitatively excluded organic Cu species as major components (Fig. 2b). The soil Cu FT spectrum was similar to Cu adsorbed on goethite, and their fitting results show very similar scattering paths (Table 3). Cu–N backscattering pairs, although indistinguishable from Cu–O pairs using EXAFS, were neglected based on the Cu  $L_{3,2}$ -edge XANES analysis

(Fig. 1b). The first shell of soil Cu was coordinated with four equatorial O atoms and one axial O atom with average Cu–O distance of  $\sim 1.96$  and  $\sim 2.24$  Å, respectively (Table 3). Similar first shell structure was also found for Cu adsorbed on goethite (Table 3). The results of soil Cu agreed well with a previous study where the average distances of  $4.5 (\pm 0.63)$  equatorial and  $1.09 (\pm 0.60)$  axial Cu–O pairs were  $\sim 1.96$  and  $\sim 2.29$  Å for Cu adsorbed on goethite with similar TOC content ( $\sim 0.55\%$ ) (Alcacio et al. 2001). Beyond the first Cu–O shell, the second shell could be modeled with 1.0 Cu/Fe atoms at  $\sim 3.04$  Å and a third shell with 1.0 Fe atoms at  $\sim 3.21$  Å. This result for our soil Cu complex is quite similar to those for Cu adsorbed on goethite with 1.0 Cu/Fe atom at  $\sim 3.07$  Å and  $\sim 1.38$  Fe atoms at  $\sim 3.28$  Å (Table 3). Cu and Fe were both reasonable as the second shell backscattering atom of soil Cu, as higher shell Fe neighbors cannot be easily distinguished from Cu because of similar backscattering amplitudes (Parkman et al. 1999). Furthermore, we interpreted the third shell neighbor atom to be Fe atom because the average distance of Cu–Fe pair with  $\sim 3.24$  Å was much longer than the reported Cu–Cu distances (2.93–3.07 Å) (Peacock and Sherman 2005). This long interatomic distance of Cu–Fe pair also accorded with the previously reported average distance (3.17–3.41 Å) of Cu–Fe pair for Cu adsorbed to Fe oxides (Alcacio et al. 2001; Peacock and Sherman 2005; Kumpiene et al. 2011).

#### $\mu$ -XRF/XANES microanalysis

The  $\mu$ -XRF map of soil microaggregates demonstrated the heterogeneous distributions of Cu, Fe, Mn, Ca, and K in the mining soil at the micro-scale (Fig. 3). For Cu, one hot spot (spot 1) and a few moderate intensity spots (spot 2 and spot 3)

**Fig. 2** The  $k^3$ -weighted Cu K-edge EXAFS spectra (a) and the corresponding Fourier transforms (FT) (b) of the mining soil and the selected Cu references. Solid line and red dotted line represent the experimental and fitting spectra, respectively; the red dashed box indicates the spectral regions of interest

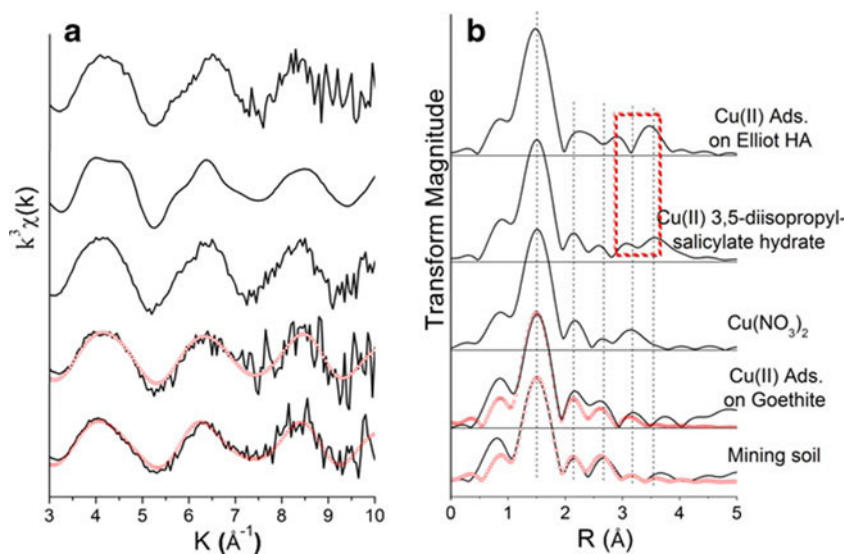


**Table 3** Fitting results of Cu K-edge EXAFS of Cu adsorbed on goethite and in the mining soil

BS <sup>a</sup>	CN <sup>b</sup>	R <sup>c</sup> (Å)	Σ <sup>2d</sup> (Å <sup>2</sup> )	ΔE <sub>0</sub> <sup>c</sup> (eV)	χ <sup>2</sup> (R) <sup>f</sup>
Cu ads. on goethite					
Cu–O <sub>eq</sub>	4 <sup>g</sup>	1.95	0.003	1.57	2.724 (0.016)
Cu–O <sub>ax</sub>	1 <sup>g</sup>	2.21	0.006 <sup>g</sup>		
Cu–Cu/Fe	1 <sup>g</sup>	3.07	0.006 <sup>g</sup>		
Cu–Fe	1.38	3.28	0.01 <sup>g</sup>		
Mining soil					
Cu–O <sub>eq</sub>	4 <sup>g</sup>	1.96	0.003	1.10	2.433 (0.006)
Cu–O <sub>ax</sub>	1 <sup>g</sup>	2.24	0.006 <sup>g</sup>		
Cu–Cu/Fe	1 <sup>g</sup>	3.04	0.006 <sup>g</sup>		
Cu–Fe	1 <sup>g</sup>	3.21	0.01 <sup>g</sup>		

<sup>a</sup> Backscattering atoms

<sup>b</sup> Coordination number

<sup>c</sup> Atomic separation distance

<sup>d</sup> Debye–Waller factor

<sup>f</sup> Fit residual

<sup>g</sup> Factors were fixed

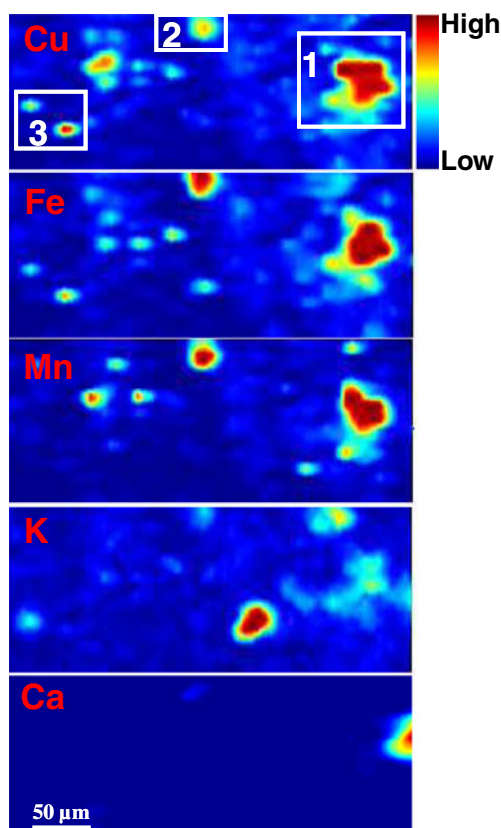
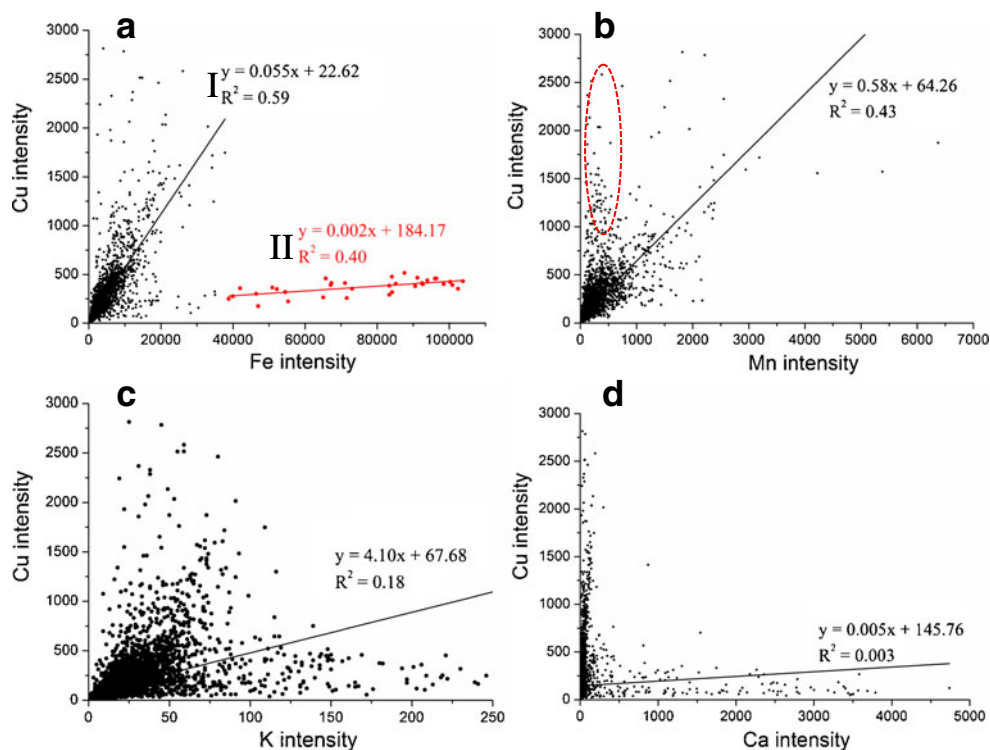


**Fig. 3** Distribution of the selected elements (Cu/Fe/Mn/K/Ca) in the thin section of the Cu mining soil sample determined by μ-XRF mapping at the micro-scale. Pixel size is 5 μm. The total map area is 0.35×0.075 mm<sup>2</sup>. Hot spot regions are marked by white boxes and labeled from 1 to 3

were found in the map with sizes ranging from a few to tens of micrometer, which indicated that a significant fraction of Cu was concentrated in isolated particles. The overlapping of Cu/Fe signals at these particles (spots 1, 2, and 3) suggested a close correlation of Cu to Fe oxides in the soil microaggregates (Fig. 3). Further regression analysis between the intensities of Cu and Fe indicated at least two distribution patterns which could be described by separate regression equations (Eqs. I and II, Fig. 4a). The majority of soil Cu highly correlated with moderate Fe intensities less than ~40,000 counts (Eq. I,  $R^2=0.59$ ), compared to the region with high Fe intensities ranging from ~40,000 to ~110,000 counts (Eq. II,  $R^2=0.40$ ; Fig. 4a). This suggested that Cu was mainly associated with Fe oxides and such association mainly occurred in the soil particles with moderate Fe contents in the mining soil. The correlation of Cu and Mn was considered to be relatively lower ( $R^2=0.43$ , Fig. 4b) because the two elements were co-distributed in the spots 1 and 2 but had no correlation at spot 3 (Fig. 3). Consistently, the majority of high Cu counts (>1,000) correlate with low Mn counts (<500), as indicated by the red line cycle area in Fig. 4b. K is used as a proxy for clay minerals in μ-XRF studies (Strawn and Baker 2008); the Cu hot spot 1 only correlated to moderate K fluorescence and had no correlation to the spot with the highest K counts (Fig. 3). There was also a relatively low regression coefficient  $R^2$  (~0.18) between K and Cu intensities (Fig. 4c). Therefore, clays appeared not to be the major sink of Cu in the soil microaggregates. Similarly, Cu hot spots were separated from the regions with significant Ca counts (Fig. 3), consistent with a rather low  $R^2$  (~0.003) for the regression equation between the intensities of Cu and Ca (Fig. 4d). This indicated that soil Cu was not associated with soil minerals containing Ca.

The μ-XANES spectrum was only successfully collected at the Cu hot spot 1 instead of moderate intensity spot 2 and spot 3 of the soil microaggregates due to detection limit (Fig. 1a). Compared to the soil Cu K-edge bulk-XANES spectrum, a new shoulder peak (peak 2) was resolved at 8,980 eV in the μ-XANES spectrum of the hot spot 1. This peak was consistent with that of Cu(0)/Cu(I) references (Cu, Cu<sub>2</sub>O, and Cu<sub>2</sub>S) in Fig. 1a, indicating the presence of soil Cu species with low oxidation states. Further analysis of the corresponding first derivative spectra suggested Cu<sub>2</sub>S was one of the most possible low valency Cu species in the mining soil, as clearly demonstrated by the well alignment of peak γ in soil μ-XANES spectrum to that of Cu<sub>2</sub>S spectrum (Fig. S1 in SM). Furthermore, another characteristic peak (peak β') of the hot spot 1 was well aligned to that of Cu<sub>2</sub>S in Fig. S1 (in SM). These confirmed that Cu<sub>2</sub>S existed in the soil, in agreement with the bulk-XANES analysis at Cu L<sub>3,2</sub>-edge, as indicated by the alignment of peaks C and D between soil spectrum and that of Cu<sub>2</sub>S (Fig. 1b). However peak α of the hot spot 1 in Fig. S1 (in SM) was absent in the spectra of Cu<sub>2</sub>S, but present

**Fig. 4** Correlation between the intensities of Cu with Fe (a), Mn (b), K (c), and Ca (d) within maps of the mining soil determined by  $\mu$ -XRF (Fig. 3); pixels of different associations between Cu and Fe (with their equations of regression and  $R^2$ ) were present in different colors. Equations I and II in Fig. 4a represent the regression equation of intensities between Cu and moderate Fe with fluorescence counts less than 40,000 and between Cu and high Fe with fluorescence counts from 40,000 to 110,000, respectively; the selected area in Fig. 4b with high Cu but low Mn was highlighted by red cycle



in soil Cu, Cu adsorbed on goethite, and humic acid, in addition that peak  $\beta$  seems partly being included in peak  $\beta'$  (Fig. S1 in SM). All these results suggested that the hot spot 1 was a mixture of  $\text{Cu}_2\text{S}$  and Cu adsorbed on Fe oxides and/or humic acid. Further LCF analysis of the soil  $\mu$ -XANES spectrum indicated the most likely Cu species were  $\text{Cu}_2\text{S}$  and Cu(II) adsorbed on goethite in Cu hot spot 1 isolated from the mining soil. The best fitting results indicated that  $\text{Cu}_2\text{S}$ , accounting for 57.8 % of total Cu, dominated in the Cu species, but Cu(II) adsorbed on goethite only had a percentage of 42.2 % of total Cu (Table 2).

#### STXM nanoanalysis

The nano-scale spatial distributions of Cu, Fe, Al, and Si in the mining soil were probed by STXM. Significant chemical heterogeneity occurred in the mining soil at the nano-scale (Figs. 5 and S3 in SM). Cu was highly concentrated in two spots (spots I and II) of the targeted microaggregates (Figs. 5a and S3a in SM), while Fe, Al, and Si were present throughout the soil (Fig. 5a, b). Fingerprint analysis of the Cu  $L_3$ -edge XANES of spot I indicated the dominance of Cu(II) in the soil as evidenced by the strong main peak ( $L_3$ -edge) in the spectrum of soil Cu (Fig. S4a in SM), although the relatively high noise in the soil Cu spectrum limited further identification of other Cu oxidation state (Fig. S4a in SM). The Fe  $L_{3,2}$ -edge XANES spectra of different spots in the microaggregates indicated the presence of both Fe(II) and Fe(III) in the soil (Fig. S4b in SM), with the majority of iron present as Fe(III)

oxides (Fig. 5c). The overlapping of Cu and Fe(III) (Fig. 5c), rather than Al and Si (Fig. 5a), in the two Cu hot spots further confirmed the dominance of Cu associated with Fe oxides, especially Fe(III) oxides. This was also supported by the highest correlation of Cu to the total Fe ( $r=0.768$ ) and much higher correlation of Cu to Fe(III) ( $r=0.757$ ) compared to Cu to Fe(II) ( $r=0.627$ ), Si ( $r=0.589$ ), and Al ( $r=0.570$ ) (Table 4). Furthermore, Si correlated well with Al in the investigated microaggregates ( $r=0.973$ ), consistent with aluminosilicate minerals present (Table 4). Fingerprint analysis of Al and Si K-edge XANES spectra of the Spot IV in the microaggregates (Fig. S4c, d) suggested muscovite was the targeted clay, which agreed with bulk soil XRD results (Table 1). In addition, the co-distribution of Cu, Fe(III), Al, and Si occurred in spot III (Fig. 5a–c) with moderate Cu concentration, in agreement with relatively high correlation of Cu–Si ( $r=0.589$ ), Cu–Al ( $r=0.570$ ), Fe(III)–Si ( $r=0.728$ ), and Fe(III)–Al ( $r=0.664$ ; Table 4). This might be the result of an association of Cu to Fe(III) oxide coatings of muscovite in the mining soil.

#### Quick-XANES diagnosis of radiation damage on soil Cu

Nineteen successive quick scans on the same spot of the mining soil at Cu L-edge gained almost the same Cu Q-XANES spectra which exhibited insignificant change in the intensities of Cu(II) peaks at 930.9 eV (peak A,  $L_3$ -edge) and 950.7 eV (peak B,  $L_2$ -edge) (Fig. 6). Furthermore, there was no significant variation in the intensity of Cu(I) peak (peak C)



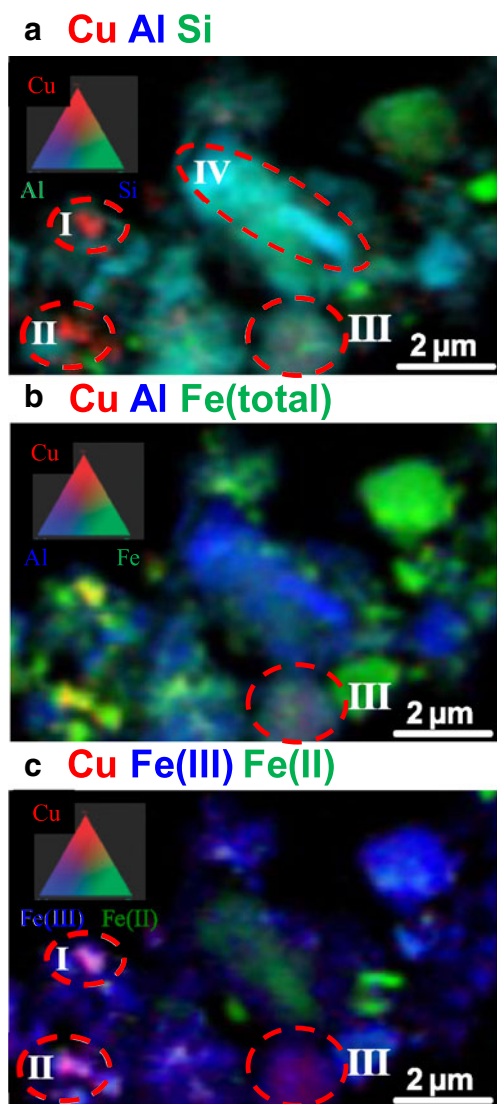


**Fig. 5** Distribution of Cu/Fe/Al/Si in the interested region of the mining soil determined by STXM at the nano-scale. Panels **a**, **b**, and **c** represent the overlapping of Cu/Al/Si, Cu/Al/Fe (total), and Cu/Fe(III)/Fe(II) mapping in the interested region, respectively. Spots of interest are indicated with red dashed circles and are labelled I–IV

at 933.9 eV among these soil Cu Q-XANES spectra (Fig. 6). Additionally, the peak features in these Cu Q-XANES spectra of the mining soil collected at SGM beamline in CLS (Fig. 6) were similar to those collected at the soft X-ray beamline in

**Table 4** Correlation coefficients (*r*) from pairs of optical density (OD) values from different elements within maps of the mining soil microaggregates analyzed by STXM

	Si	Al	Fe(III)	Fe(II)	Fe(total)
Cu	0.589	0.570	0.757	0.627	0.768
Si		0.973	0.728	0.700	0.757
Al			0.664	0.655	0.689

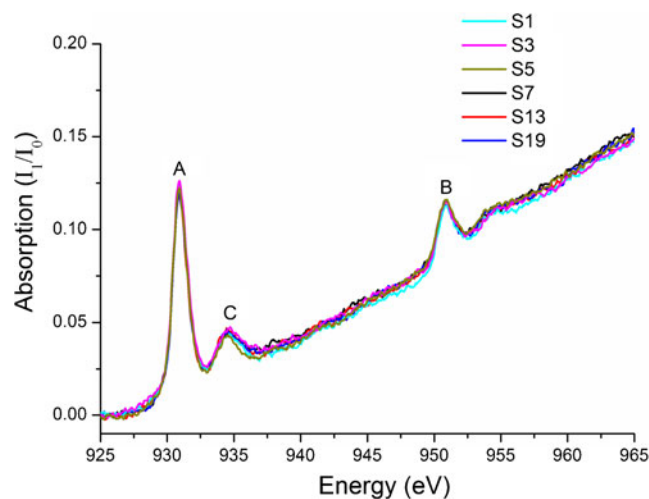


**Fig. 6** The selected Cu L<sub>3</sub>-edge XANES spectra of the mining soil under 19 successive fast scans. The listed numbers (1 to 19) represent the 1st to 19th scan (S1 to S19)

BSRF (Fig. 1b) where photoreduction of organic Cu(II) complexes did not occur during Cu L<sub>3,2</sub>-edge XANES measurement as result of low beam intensity of ~10<sup>8</sup> photons/s (Yang et al. 2011). Therefore, we conclude that radiation damage did not occur in these Cu Q-XANES measurements of the mining soil, and instead a low oxidation state Cu species (most likely Cu<sub>2</sub>S) is present.

**Discussion**

Soil Cu sequestration by Fe(III) oxides

The investigated Cu-contaminated mining soil contains quartz, kaolinite, clinocllore, and muscovite according to XRD data analysis (Table 1). The possibility of crystalline Cu minerals in the soil can be eliminated due to their absence in XRD measurements. Instead, the dominant species present is the association of Cu with Fe oxides: this is consistently observed at the molecular level via both bulk spectroscopy (Cu K-edge bulk-XANES and bulk-EXAFS) and micro-/nano-scale microscopy (μ-XRF and STXM). Similar peak features between soil Cu and Cu adsorbed on goethite occurred in the Cu K-edge bulk-XANES spectra (Figs. 1a and S1 in SM) and the FT of bulk-EXAFS spectra (Fig. 2), in agreement with the highest correlation of Cu to Fe in the micro-scale μ-XRF (Figs. 3 and 4) and nano-scale STXM analysis of the mining soil (Fig. 5b and Table 4). LCF analysis of soil Cu bulk-XANES spectra estimated 81 % of Cu in the soil adsorbed on Fe oxides (Table 2). Consistently, fine fitting of soil Cu bulk-EXAFS spectra revealed the coordinated Fe atoms at the second and third shells (Table 3), which accorded with the previous reports on Cu sorbed to Fe oxides under different pH value (Parkman et al. 1999; Peacock and

Sherman 2005). Therefore, Cu mainly adsorbed to Fe oxides by inner-sphere complexation in the soil. This generally agreed with the low content of SOM, but high concentration of Fe in the mining soil (Table 1), because Fe oxides are the second most important soil sorbent for Cu (behind SOM) (Vega et al. 2006). Although it is known that SOM has an affinity for coating Fe oxide minerals, Cu may also form ternary complexes bonding to both SOM and Fe oxides (Alcacio et al. 2001; Strawn and Baker 2009); this is unlikely in the mining soil according to the lack of multiple scattering Cu–C–O EXAFS features in the soil FT spectra (Fig. 2b). This was also supported by the absence of Cu photoreduction for this soil using successive Q-XANES measurements (Fig. 6); organic Cu(II) complexes are very sensitive to photoreduction when exposed to high-intensity X-ray beam (Strawn and Baker 2008; Manceau and Matynia 2010; Yang et al. 2011). These results for a Chinese mining soil are quite different from previous findings that Cu(II) was mainly complexed with SOM in contaminated agricultural soils (Jacobson et al. 2007; Strawn and Baker 2008, 2009). Such discrepancy may mainly arise from the much higher SOM content in previous studies (2.2~75 %) compared to our soil (~0.55 %) since it is known that low SOM content facilitated Cu to adsorb on mineral surface (Alcacio et al. 2001; Strawn and Baker 2009).

Mn oxides, Ca minerals, and clays, although potential sinks of soil Cu (Strawn and Baker 2009), were not important in the Cu speciation of our mining soil. The  $\mu$ -XRF analysis indicated that a minor amount of Cu may be associated with Mn oxides, possibly because Mn oxides generally coexist with Fe oxides as ferromanganese nodules in soils (Manceau et al. 2003). However, little Cu was sorbed to minerals containing Ca in the mining soil based on the  $\mu$ -XRF analysis (Figs. 3 and 4). Muscovite clays rich in Al and Si were observed in STXM mapping (Fig. 5a, spots III and IV); a lack of both Cu and Fe(III) signals in the spot IV suggested that the muscovite without Fe(III) oxides adsorbed little Cu, while the co-distribution of Cu and Fe(III) in the spot 3 indicated muscovite with Fe(III) oxides could adsorb Cu (Fig. 5c). This further refines the bulk and micro-scale measurements that showed Cu association with Fe(III) oxides rather than clays; in fact, clays with Fe oxide coatings could be an important Cu sink. This also probably accounted for the  $\mu$ -XRF results of the Cu hot spot 1, which only had moderate K fluorescence, but did not correlate to the spot with the highest K counts (Figs. 3 and 4). In the mining soil, Cu was mainly associated with Fe(III) oxides rather than Fe(II) oxides (Fig. 5c), and such Fe(III) oxides were distributed as isolated particles (spot I and spot II) or as coatings on clays (spot III) according to the STXM analysis (Fig. 5).

Overall, the bulk, micro, and nano-scale speciation all confirmed that Cu is associated with Fe oxides rather than SOM and clay minerals in the mining soil, although only one soil sample was analyzed in detail by multiple

synchrotron-based techniques over a range of spatial scales. These results strongly imply a natural sequestration of Cu by Fe oxides in the mining site. As Cu stability may be sensitive to redox changes due to reductive dissolution of Fe(III) oxides, engineering measures (e.g., good drainage) are needed to keep oxidic soil conditions for Cu sequestration at the studied mining site.

#### Characterization of soil Cu(I) by XANES

Fingerprint analysis of peak 2 in the Cu K-edge  $\mu$ -XANES spectrum of the mining soil revealed the presence of low oxidation state of Cu(I), probably as  $\text{Cu}_2\text{S}$ , in the mining soil (Fig. 1a, b), which was distinguished from the absence of visible peak 2 in soil Cu K-edge bulk-XANES spectra that suggested the soil only contained Cu(II) species (Fig. 1a). Previous study indicated that soil Cu(I) observed in micro-probe experiments may be radiation-damage artifacts as a result of X-ray-induced photoreduction of Cu(II) to Cu(I) in organic Cu(II) compounds or Cu(II) complexes with SOM in contaminated soil (Strawn and Baker 2008; Manceau and Matynia 2010). Recently, we found that photoreduction of organic Cu(II) complexes during each Cu  $L_{3,2}$ -edge XANES measurement mainly resulted from the high radiation dose, which highly correlated with beam intensity (Yang et al. 2011). With comparative beam intensity at SGM beamline ( $10^{10}$ ~ $10^{11}$  photons/s) to 15U beamline ( $\sim 10^{10}$  photons/s), 19 continuous repeated Q-XANES measurements on the same spot of the mining soil obtained the same Cu  $L_{3,2}$ -edge XANES spectra without any significant change in the intensities of Cu(II) peaks (peak A, peak B) and Cu(I) peak (peak C) among these scans (Fig. 6). These results are in contrast with our previous study in which radiation damage of organic Cu(II) complexes gradually reduces Cu(II) peak intensity, but enhances Cu(I) peak intensity after long-term successive normal scans at this beamline (Yang et al. 2011). As Cu  $L_{3,2}$ -edge Q-XANES spectroscopy highly reduced scan time (20 s) compared to normal scan (5 min) at this beamline, each Cu Q-XANES spectrum of the investigated mining soil could minimize radiation damage to the maximum extent at the current level of the beamline instrumentation. Therefore, radiation damage is unlikely to be responsible for Cu(I) in our Cu  $L_{3,2}$ -edge Q-XANES spectra, and the Cu  $\mu$ -XANES spectrum of the mining soil should be free from beam-catalyzed photoreduction.

The best LCF results of soil Cu K-edge  $\mu$ -XANES spectrum in spot 1 consisted of  $\text{Cu}_2\text{S}$  (57.8 % of total Cu) and Cu adsorbed on goethite (42.2 % of total Cu) (Fig. 6b); this is also in agreement with the fingerprint analysis of soil  $\mu$ -XANES derivative spectrum (Fig. S1 in SM). Although Cu K-edge  $\mu$ -XANES spectrum was only successfully collected at one Cu hot spot 1, the LCF results of soil  $\mu$ -XANES spectrum were also qualitatively verified by soil Cu K-edge and  $L_{3,2}$ -edge

bulk-XANES results. Indeed, soil Cu bulk-XANES analysis at K-edge and L-edge both indicated the presence of Cu<sub>2</sub>S in the mining soil (Table 2 and Figs. 1b and S2a in SM); meanwhile, LCF analysis of soil Cu K-edge bulk-XANES spectrum showed Cu adsorbed on goethite (81.6 % of total Cu) dominated in the mining soil (Table 2 and Fig. S2b in SM). Because soil Cu bulk-XANES analysis provided averaged Cu speciation information of targeted sample area at millimeter (1–3 mm) spatial scales, this may be more representative of Cu speciation in the mining soil. Therefore, this study strongly suggested the true presence of Cu(I) as Cu<sub>2</sub>S enriched in some isolated microaggregates of the mining soil, although Cu, mainly present as Cu(II), primarily sequestered by Fe oxides in the bulk soil. Favas et al. (2011) also found that a certain amount of Cu existed as primary sulfides, as well as a primary Cu–Fe oxide association in mining soils subjected to selective chemical extraction. As Cu<sub>2</sub>S is widely distributed in Cu mining sites (Todd and Sherman 2003), it is reasonable to infer that Cu<sub>2</sub>S probably existed in Cu sulfides of the mining soil fractionated by selective chemical extraction. The highly localized Cu<sub>2</sub>S (57.8 %) in isolated microaggregate of the mining soil suggests that this phase may play an important role in speciation and solubility in certain microsites of mining soils even when the general sequestration of Cu by Fe oxides in the bulk soil dominates. Such mismatch of Cu speciation between soil microsite and bulk soil is consistent with the recent “soil microreactor concept” proposed by Hesterberg et al. (2011) who argue each soil microsite may behave as unique micro- or nanoreactor for soil contaminants, and thus, microscale understanding of soil chemistry is necessary for predicting contaminant reactivity and environmental fate in soils. Additionally, the detection of soil Cu(I) in the bulk L-edge measurements highlights the higher sensitivity of bulk-XANES spectroscopy at the Cu L-edge than the Cu K-edge to characterize the oxidation state of soil Cu. This agrees with the high intensity of the dipole-transition (Cu 2p→3d) peak in the Cu L<sub>3,2</sub>-edge XANES spectra compared to that of Cu K-edge XANES spectra in which Cu 1s→3d transition is dipole forbidden (Shimizu et al. 2001; Solomon et al. 2005).

## Conclusions

In this study, although only one soil sample was investigated, new molecular-level evidence of general Cu sequestration by Fe oxides in contaminated soil over a range of spatial scales was obtained using multiple complementary synchrotron-based bulk and microscopic techniques. The high degree of localization of Cu<sub>2</sub>S in soil microaggregate by μ-XANES analysis, distinguished from bulk soil Cu speciation, suggested the uniqueness of Cu transformation involving S cycling in certain microsites of the mining soil. Considering the microscale heterogeneities in soil with unique chemical

microenvironments, we foresee future wide application of spatially resolved techniques (μ-XRF, μ-XANES, STXM, etc.) for speciating heavy metals in contaminated soils, although radiation damage due to brilliant microfocus X-ray beam should be considered and monitored. The widely established impact of sulfur on heavy metal speciation through forming metal sulfide (e.g., soil Cu<sub>2</sub>S found in this study) calls for high-sensitivity detection capacity of S in heavy metal-contaminated soils during μ-XRF and STXM mapping. Finally, the higher sensitivity of XANES spectroscopy at Cu L-edge compared to the K-edge suggests further potential application of 3d transition metal L-edge XANES capabilities to probe heavy metal speciation in the contaminated soils. Overall, while this study, taking a single mining soil as an example, demonstrates the great advantages of using combined multiple synchrotron-based bulk and microscopic techniques in characterizing Cu distribution and speciation in contaminated soil, further examination of many soils with these techniques is required to fully understand Cu behavior in the soils of mining sites.

**Acknowledgments** We thank Prof. Yuying Huang and Xiaohan Yu at the SSRF and Dr. Yidong Zhao at the BSRF for their kind help during these synchrotron experiments. This research was funded by the National Natural Science Foundation of China (21207114, 11179025); China Postdoctoral Science Foundation (2012M511375); Zhejiang Provincial Natural Science Foundation of China (R5110031); and Program for New Century Excellent Talents in University (NCET-11-0455). Cu L<sub>3,2</sub>-edge XANES and STXM measurements were performed at the SGM and Spectromicroscopy beamlines in CLS which was supported by NSERC, NRC, CIHR, the Province of Saskatchewan, WEDC, and the University of Saskatchewan.

## References

- Alcacio TE, Hesterberg D, Chou JW et al (2001) Molecular scale characteristics of Cu(II) bonding in goethite-humate complexes. *Geochim Cosmochim Acta* 65:1355–1366
- Boudesocque S, Guillon E, Aplincourt M et al (2007) Sorption of Cu(II) onto vineyard soils: macroscopic and spectroscopic investigations. *J Colloid Interface Sci* 307:40–49
- Boularbah A, Schwartz C, Bitton G et al (2006) Heavy metal contamination from mining sites in South Morocco: 1. Use of a biotest to assess metal toxicity of tailings and soils. *Chemosphere* 63:802–810
- Brown GE, Catalano JG, Templeton AS et al (2005) Environmental interfaces, heavy metals, microbes, and plants: applications of XAFS spectroscopy and related synchrotron radiation methods to environmental science. *Phys Scr T* 115:80–87
- Chen X, Shi J, Chen Y et al (2006) Tolerance and biosorption of copper and zinc by *Pseudomonas putida* CZ1 isolated from metal-polluted soil. *Can J Microbiol* 52:308–316
- Croue JP, Benedetti MF, Violleau D et al (2003) Characterization and copper binding of humic and nonhumic organic matter isolated from the South Platte River: evidence for the presence of nitrogenous binding site. *Environ Sci Technol* 37:328–336
- Dynes JJ, Tylliszczak T, Araki T et al (2006) Speciation and quantitative mapping of metal species in microbial biofilms using scanning transmission X-ray microscopy. *Environ Sci Technol* 40:1556–1565

- Elguindi J, Hao XL, Lin YB et al (2011) Advantages and challenges of increased antimicrobial copper use and copper mining. *Appl Microbiol Biotechnol* 91:237–249
- Favas PJC, Pratas J, Gomes MEP et al (2011) Selective chemical extraction of heavy metals in tailings and soils contaminated by mining activity: environmental implications. *J Geochem Explor* 111:160–171
- Fittschen UEA, Falkenberg G (2011) Trends in environmental science using microscopic X-ray fluorescence. *Spectrochim Acta B At Spectrosc* 66:567–580
- Flogeac K, Guillon E, Aplincourt M (2004) Surface complexation of copper(II) on soil particles: EPR and XAFS studies. *Environ Sci Technol* 38:3098–3103
- Frenkel AI, Korshin GV, Ankudinov AL (2000) XANES study of Cu<sup>2+</sup> binding sites in aquatic humic substances. *Environ Sci Technol* 34:2138–2142
- Griioni M, Goedkoop JB, Schoorl R et al (1989) Studies of copper valence states with Cu L<sub>3</sub> X-ray-absorption spectroscopy. *Phys Rev B* 39:1541–1545
- Guo GY, Yuan T, Wang WH et al (2011) Bioavailability, mobility, and toxicity of Cu in soils around the Dexing Cu mine in China. *Environ Geochem Health* 33:217–224
- Hesterberg D, Duff MC, Dixon JB et al (2011) X-ray microspectroscopy and chemical reactions in soil microsites. *J Environ Qual* 40:667–678
- Hitchcock AP, Dynes JJ, Lawrence JR et al (2009) Soft X-ray spectromicroscopy of nickel sorption in a natural river biofilm. *Geobiol* 7:432–453
- Jacobson AR, Dousset S, Andreux F et al (2007) Electron microprobe and synchrotron X-ray fluorescence mapping of the heterogeneous distribution of copper in high-copper vineyard soils. *Environ Sci Technol* 41:6343–6349
- Karlsson T, Persson P, Skyllberg U (2006) Complexation of copper(II) in organic soils and in dissolved organic matter—EXAFS evidence for chelate ring structures. *Environ Sci Technol* 40:2623–2628
- Kumpiene J, Mench M, Bes CM et al (2011) Assessment of aided phytostabilization of copper-contaminated soil by X-ray absorption spectroscopy and chemical extractions. *Environ Pollut* 159:1536–1542
- Lawrence JR, Dynes JJ, Korber DR et al (2012) Monitoring the fate of copper nanoparticles in river biofilms using scanning transmission X-ray microscopy (STXM). *Chem Geol* 239:18–25
- Liu SH, Wang HP (2004) In situ speciation studies of copper-humic substances in a contaminated soil during electrokinetic remediation. *J Environ Qual* 33:1280–1287
- Lu RK (1999) Analytical methods of soil and agricultural chemistry. China Agricultural Science and Technology, Beijing
- Manceau A, Matynia A (2010) The nature of Cu bonding to natural organic matter. *Geochim Cosmochim Acta* 74:2556–2580
- Manceau A, Marcus MA, Tamura N (2002) Quantitative speciation of heavy metals in soils and sediments by synchrotron X-ray techniques. *Rev Mineral Geochem* 49:341–428
- Manceau A, Tamura N, Celestre RS et al (2003) Molecular-scale speciation of Zn and Ni in soil ferromanganese nodules from loess soils of the Mississippi Basin. *Environ Sci Technol* 37:75–80
- Morton JD, Semrau JD, Hayes KF (2001) An X-ray absorption spectroscopy study of the structure and reversibility of copper adsorbed to montmorillonite clay. *Geochim Cosmochim Acta* 65:2709–2722
- Parkman RH, Charnock JM, Bryan ND et al (1999) Reactions of copper and cadmium ions in aqueous solution with goethite, lepidocrocite, mackinawite, and pyrite. *Am Mineral* 84:407–419
- Peacock CL, Sherman DM (2005) Copper(II) sorption onto goethite, hematite, and lepidocrocite: a surface complexation model based on ab initio molecular geometries and EXAFS spectroscopy. *Geochim Cosmochim Acta* 69:5141–5142
- Ravel B, Newville M (2005) ATHENA, ARTEMIS, HEPHAESTUS: data analysis for X-ray absorption spectroscopy using IFEFFIT. *J Synchrotron Radiat* 12:537–541
- Regier T, Krochak J, Sham TK et al (2007) Performance and capabilities of the Canadian Dragon: the SGM beamline at the Canadian Light Source. *Nucl Instrum Meth A* 582:93–95
- Schofield PF, Henderson CMB, Cressey G et al (1995) 2p X-ray absorption spectroscopy in the earth sciences. *J Synchrotron Radiat* 2:93–98
- Shi JY, Wu B, Yuan XF et al (2008) An X-ray absorption spectroscopy investigation of speciation and biotransformation of copper in *Elsholtzia splendens*. *Plant Soil* 302:163–174
- Shimizu K, Maeshima H, Yoshida H et al (2001) Ligand field effect on the chemical shift in XANES spectra of Cu(II) compounds. *Phys Chem Chem Phys* 3:862–866
- Solomon EI, Hedman B, Hodgson KO et al (2005) Ligand K-edge X-ray absorption spectroscopy: covalency of ligand-metal bonds. *Coord Chem Rev* 249:97–129
- Strawn DG, Baker LL (2008) Speciation of Cu in a contaminated agricultural soil measured by XAFS,  $\mu$ -XAFS, and  $\mu$ -XRF. *Environ Sci Technol* 42:37–42
- Strawn DG, Baker LL (2009) Molecular characterization of copper in soils using X-ray absorption spectroscopy. *Environ Pollut* 157:2813–2821
- Todd EC, Sherman DM (2003) Surface oxidation of chalcocite (Cu<sub>2</sub>S) under aqueous (pH = 2–11) and ambient atmospheric conditions: mineralogy from Cu L- and O K-edge X-ray absorption spectroscopy. *Am Mineral* 88:1652–1656
- USDA (1988) Soil taxonomy: a basic system of soil classification for making and interpreting soil surveys. Krieger, Florida
- Vega FA, Covelo EF, Andrade M (2006) Competitive sorption and desorption of heavy metals in mine soils: influence of mine soil characteristics. *J Colloid Interface Sci* 298:582–592
- Wan J, Tylliszczak T, Tokunaga TK (2007) Organic carbon distribution, speciation, and elemental correlations within soil micro aggregates: applications of STXM and NEXAFS spectroscopy. *Geochim Cosmochim Acta* 71:5439–5449
- Yang JJ, Regier T, Dynes JJ et al (2011) Soft X-ray induced photoreduction of organic Cu(II) compounds probed by X-ray absorption near-edge (XANES) spectroscopy. *Anal Chem* 83:7856–7862